

Wireless Sensor Network: Channel Propagation Measurements and Comparison With Simulation

Weilian Su and Mohamad Alzaghal
Naval Postgraduate School
Department of Electrical and Computer Engineering
Monterey, CA 93943
USA

Abstract: Wireless Sensor Networks (WSNs) is an important field of study as more and more applications are enhancing daily life. The technology trend is to achieve small-sized, cheap, and power efficient sensor nodes, which will make the system reliable and efficient. The Crossbow Technologies MICAz mote is an example used in this paper. Measurements of its propagation characteristics in a realistic environment will help the deployment and installation of these motes to form a WSN. The CST Microwave Studio is used to build a simulation of the MICAz. The results and comparisons between empirical and simulated data are intended to assist in the design, future studies and deployment of WSNs in the real world.

Key-Words: Wireless Sensor Networks, Propagation Characteristics, MICAz Motes

1 Introduction

The Wireless Sensor Network (WSN) technology is not a new concept; military applications have long been used for surveillance and data collection. A recent boost of interest in this technology and its applications results from the advance in the Micro-Electromechanical System (MEMS) making the fabrication of small-sized and cheap sensor nodes feasible.

Sensor nodes, or motes as many call them, are small-sized sophisticated sensors with the ability to be connected to each other. These motes could be deployed randomly using artillery or parachutes in the military domain. Another deployment method is to install the motes at specific location to get the best coverage and connectivity.

Sensor nodes are required to have many functions. Even though they are tiny, they should be able to sense the phenomenon (temperature, light, pressure, etc.), and at the same time communicate with each other, with a base station, or with a cluster head.

Some applications require the WSN deployment to be widely spread, thus making its implementation more challenging. Sensor nodes should balance between the limited storage capacity and aggregation of data gathered to reduce congestion.

The assumption that the range of the sensor nodes is uniform and homogeneous does not echo the real behavior of the network with respect to power transmitted and received, which will affect the deployment and implementation of the WSN.

Although our study is focused on Crossbow Technologies MICAz sensor motes, many of the results are applicable to other platforms and systems and hopefully are useful for the design and implementation of the WSN.

The objective of our work is to investigate the irregularity of the range and other propagation characteristics of the MICAz motes. This is primarily due to the complex propagation environment in which the WSN operates. Testing and evaluation of these motes at the system-level were conducted. The results were analyzed and compared with simulations.

The paper is divided into five sections. Section 2 discusses the related work in wireless sensor networks. RF characteristics of sensor nodes and MICAz mote specifications are presented in Section 3. The experimental setup and simulation are described in Section 4. Lastly, we conclude in Section 5.

2 Related Work

Recently, some research efforts focus on the propagation modeling issues of WSNs. Part of the research is concentrated on the non-isotropic pattern phenomenon of the electromagnetic radiation field around the motes. Several authors [1, 2, 3] presented the problem and proposed solutions for it using empirical data and simulation techniques. They suggested the use of specific protocols and algorithm to cope with the non-uniform field measured around the motes.

In [1], Zhou, He, Krishnamurthy, and Stankovic discuss the impact of radio irregularity on the implementation of the WSN. They presented factors that create this phenomenon such as variance in the Radio Frequency (RF) transmitting power and different path losses of propagation. They established a radio model for simulation and called it the Radio Irregularity Model (RIM) to bridge the discrepancy between spherical radio models used by simulators and the physical reality of radio signals. They introduced six practical solutions for radio irregularity.

Radio channel models are presented in a general context in [3]. Zhon, Das, and Gupta evaluated and approximated radio coverage around the node. They measured the interference of the systems and introduced a "Disk Model" to approximate the radiation pattern, which is not always an accurate approximation.

Kotz, Newport, and Elliott [2] discussed the mistaken assumptions in wireless network research regarding the non-uniform field and asymmetric non-reciprocal field strength in both directions between the receiver and transmitter. The author focused on 802.11 wireless systems while this paper will focus on 802.15 systems such as the WSN.

Other studies discussed the effect of transmission radius in wireless networks. In [4] and [5], Gupta and Sanchez analyzed the critical transmission range to maintain connectivity in wireless networks. In [4], Gupta presented a statistical analysis of the probability of connectivity and in [5], Sanchez provided a separate algorithm to establish this connectivity.

3 WSN Antennas and MICAz mote

3.1 Antennas

In the past, antennas were considered to be a secondary component for the sensor node. Recently, more attention is directed toward the design and implementation of the antennas. Antennas should cope with the small size of the node, which makes its implementation difficult. [6]

A physically small antenna design is possible when a high frequency is used. However, the difficulty arises when the frequency of operation is relatively low. In this case, electrically small antennas must be used.

Directivity is generally not required for the WSN since the network is most likely to be deployed randomly. On the other hand, efficiency is an important design characteristic in WSN applications. To enhance efficiency, the impedance of the antenna and transmitter or receiver should be matched. The gain is directly proportional to the efficiency and the di-

rectivity characteristics of the antenna. As will be seen, when efficiency is low, the range will be less, so more power must be transmitted, or a more sensitive receiver must be used. [7]

Conducting and dielectric objects near the antenna could lower efficiency and influence the pattern thus causing deviation from isotropic. All antennas possess a property called the "keep out" region. Batteries, displays, sensors, and circuit boards should not be in this near-field region, which is calculated as $\lambda/2\pi$ of the antenna [7]. At 2.4 GHz, the near-field region is almost 2 cm in radius. The antenna designer should consider this problem in the case of the WSN. Some measures taken include placing the batteries and other metal objects as far as possible from the antenna.

For small antennas, size, efficiency and bandwidth are related to each other as follows [7]:

$$BW = \frac{2(2\pi d/\lambda)^3}{\eta} \tag{1}$$

where BW is the maximum instantaneous fractional bandwidth; $2d$ is the maximum dimension of the antenna; λ is the wavelength in meters; and η is the antenna efficiency which can be defined as the quotient of the power radiated by the antenna and the power into the antenna.

3.2 MICAZ Motes Specifications

The common components of the sensor node are sensing unit, analog digital converter, central processing unit, transceiver unit, and power unit. The Crossbow Company produces several motes: MICA, MICA2, MICA2DOT, and MICAz. Figure 1 shows a picture of the MICAz mote, which uses a Chipcon CC2420 Processor/Radio Transceiver module and follows the IEEE 802.15.4 and ZigBee Alliances at 2.4 GHz. The data rate is 250 kbps using a Direct Sequence Spread Spectrum (DSSS). The coordinate system used for pattern measurements in this paper is also shown in Figure 1.

The processor runs an open source TinyOS operating system. The module comes with memory to store up to 100,000 measurements. Also, this module is capable of over-the-air reprogramming and possesses a battery power source with the possibility of an external power supply connection.

The MICAz CC2400 radio is capable of tuning within the IEEE 802.15.4 channels, which start from 2.405 GHz to 2.480 GHz with a 5 MHz separation. The 2.405 GHz channel is selected by default.

RF transmission power can be programmed from 0 dBm to -25 dBm. It is preferable to choose the lowest transmission power, as it will reduce the interfer-

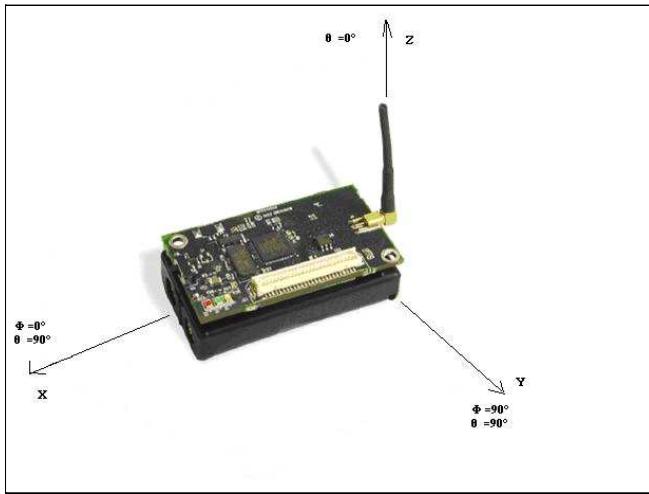


Figure 1: Photo of the MPR2400-MICAz with standard antenna.

ence and power consumption. Low power transmission keeps the range small, which reduces the probability of interference between motes. The RF Received Signal Strength Indication (RSSI) could be read directly from the CC2420 radio.

The regular antenna used with the MICAz mote is a $\lambda/4$ long insulated wire, which is called a monopole antenna. The length of the antenna operating at 2.4 GHz is 1.2 inches.

4 Experimental Setup and Simulation

Empirical data gathered using measurements in a real world environment and in a controlled environment such as an Anechoic Chamber will be compared with simulations created by software suite such as CST Microwave Studio. This section presents the techniques and assumptions for these measurements and simulations.

4.1 MICAz Antenna Pattern Measurements in Free Space

A radiation pattern is an important factor in antenna design. Some antenna parameters such as gain, half-power bandwidth, and side lobe level were determined by both simulation and measurement of the radiation pattern of the MICAz mote. An absorber lined room is used to maximize the measurement precision. In our work, the measurements occurred in the Anechoic Chamber, which located in the Spanagel Hall. To reduce reflections, the absorbers are mounted on the floor, ceiling, and the walls. These absorbers reduce

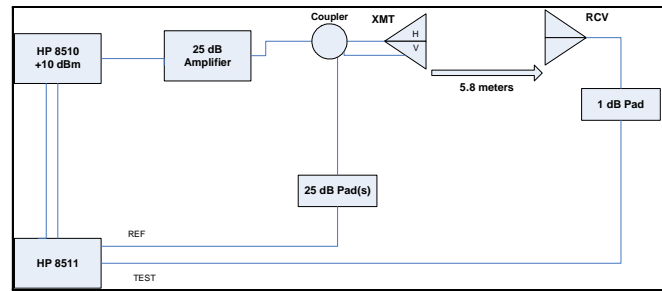


Figure 2: Block diagram of the anechoic chamber.

reflection and attenuate fields, which will reduce multipath. The chamber design should duplicate the outdoor free space propagation environment.

Figure 2 depicts the block diagram of the Anechoic Chamber antenna measurement system. The chamber is equipped with HP 8510, HP 8511, a coupler, and amplifiers. The equipment measures the transmitted power from transmitter to receiver and compares it to the power from a standard gain antenna. The distance between the transmitter and receiver is equal to 5.8 meters.

The antenna radiation pattern and gain are important aspects of the MICAz motes discussed in this section. In the first measurement, the free space radiation pattern of the mote is to be determined.

A prototype of the MICAz was built to mount the mote's monopole antenna. An adaptor is used to connect the antenna to the measurement platform. The Automated Antenna Pattern Measurement Software installed in the chamber's equipment performs the measurements automatically and the results are gathered into an output file for analysis.

A horn antenna is used at the transmitter side with 2.48 GHz frequency. The MICAz mote prototype is on the receiving side, which is rotated by the system automatically during the measurement to obtain a 360° pattern. The measurements are repeated for the horizontal orientation of the transmitting and receiving antennas.

The MICAz model is raised one meter above the floor, which is absorber lined to minimize the ground plane interference. In this study, the ground plane effect is ignored. Also, only the principal polarization was measured; no cross-polarized patterns were measured. The mount only rotates in azimuth (the horizontal plane).

The antennas were deployed in four positions as seen in Figure 3. Part (a) is a horizontal cut (x-y plane); part (b) is a vertical cut (y-z plane); part (c) is vertical cut (x-z plane with tilt to the right); and part (d) is vertical cut (x-z plane with tilt to the left). The purpose of the tilt was to identify any chamber

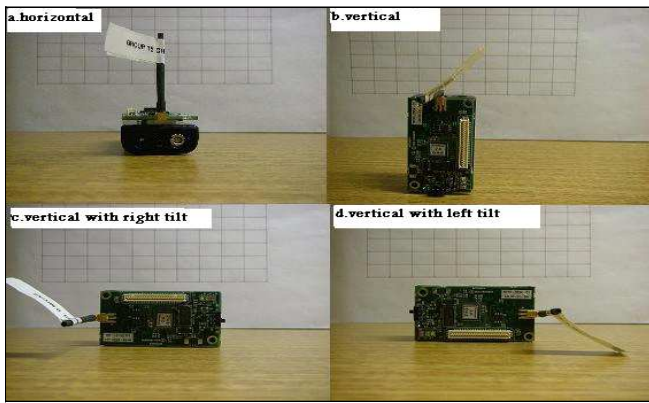


Figure 3: Multiple test position for the MICAz mote, (a) horizontal cut plane, (b) vertical cut plane, (c) vertical cut plane with right tilt, and (d) vertical cut plane with left tilt.

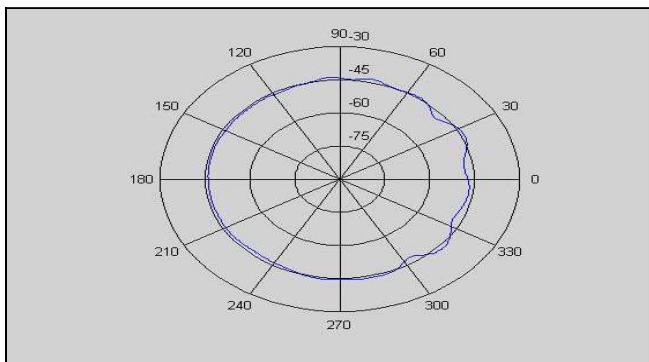


Figure 4: Pattern shows the horizontal cut plane of the measurements.

reflections in the pattern.

The output file for the first position measurements was processed using MATLAB software. Figure 4 shows the diagram of the horizontal cut of the measurements. The radial units are the received power in dBm. It shows that the pattern is almost omnidirectional for the monopole antenna. By substitution with a reference antenna, the gain was found to be approximately 0 dBi.

The graph in Figure 4 shows that the MICAz radiation pattern is uniform to within a couple of dBm. The ripple on the right hand side is due to the metallic board of the mote and the edge location of the antenna contributes to the non-uniform behavior of the pattern. In the second setup as shown in Figure 3.b, the vertical cut plane is measured following the same technique used in the first part of the experiment. Figure 5 depicts the graph of these measurement results. The radiation pattern in this case is different as it shows the characteristic nulls (notches) of the monopole antenna.

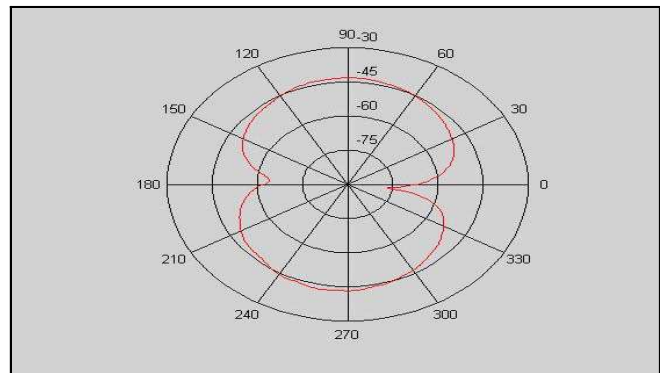


Figure 5: Pattern shows the vertical cut plane of the measurements.

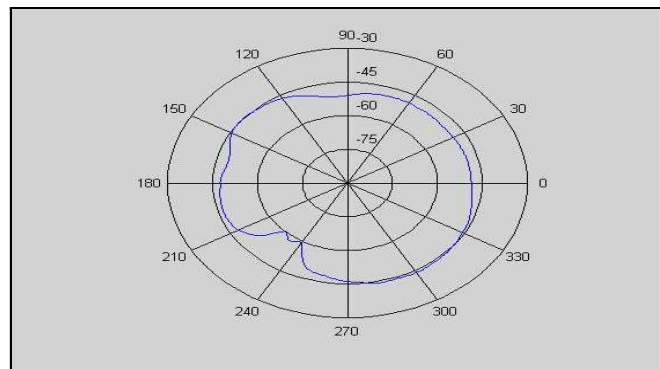


Figure 6: Pattern shows the vertical cut plane with right tilt of the measurements.

To explore the effects of chamber reflections on the vertical cut plane more in depth, the third and fourth experimental setups are conducted according to Figures 3.c and 3.d.

These two experiments were done in different tilt directions. Measurement results are shown in Figures 6 and 7. These graphs show a similar radiation pattern with a 90° rotation. They show a more uniform pattern resulting from the reduced effect of the mote board. The two experiments, which created Figures 6 and 7, resulted from two positions in the Anechoic Chamber. Ideally, the two patterns should be identical if rotated by the tilt angle. Any difference is due to reflections from the chamber walls, which change with tilt angle. The gain in cases 3.b, 3.c, and 3.d is slightly more than zero due to the effect of the mote board position with respect to the antenna.

4.2 Simulation for MICAz Mote Antenna

To simulate the MICAz mote in free space, a numerical electromagnetic code was used. Microwave Studio by Computer Simulation Technology (CST) is a tool for fast and accurate 3D EM simulation of high

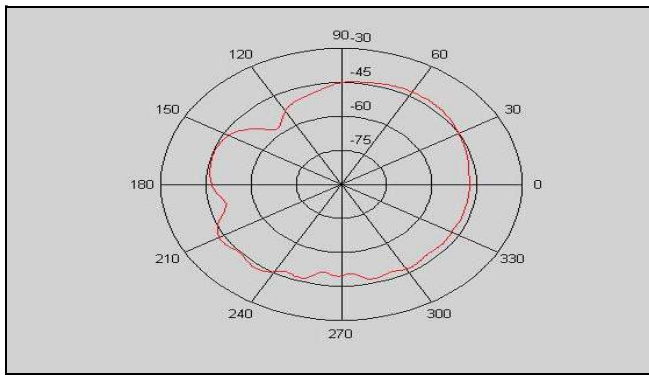


Figure 7: Pattern shows the vertical cut plane with left tilt of the measurements.

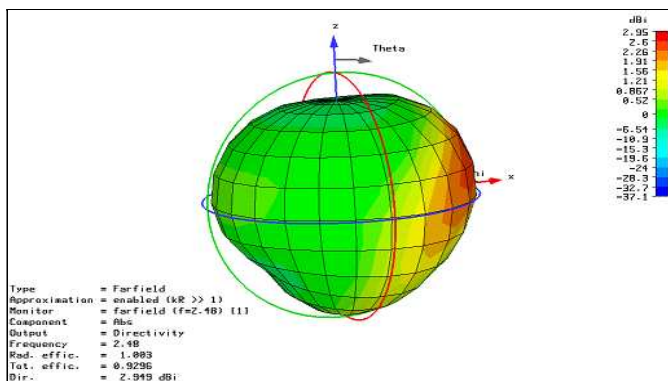


Figure 8: 3-D radiation pattern of the MICAz mote.

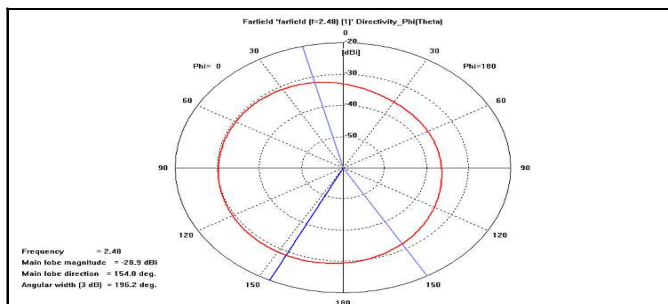


Figure 9: The radiation pattern of the horizontal plane.

frequency problems. Along with a broad application range, the CST Microwave Studio offers a considerable product to market advantages such as shorter development cycles, virtual prototyping before physical trials, and optimization instead of experimentation. It uses the finite element method and therefore is capable of computing the effects of objects in the antenna's near field.

The MICAz mote model was built using this simulator to demonstrate its radiation pattern. The dimensions of the simple MICAz model are the same as the actual dimensions of the mote, which are 56 mm on

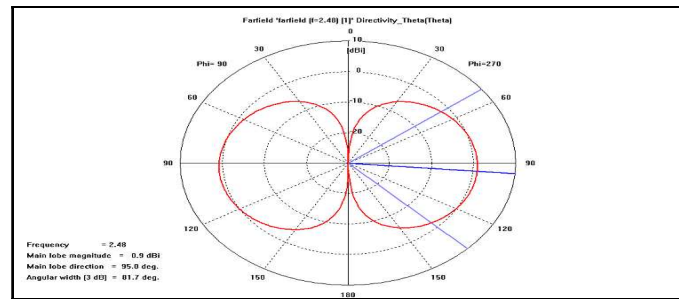


Figure 10: The radiation pattern of the vertical plane ($\Phi = 90^\circ$).

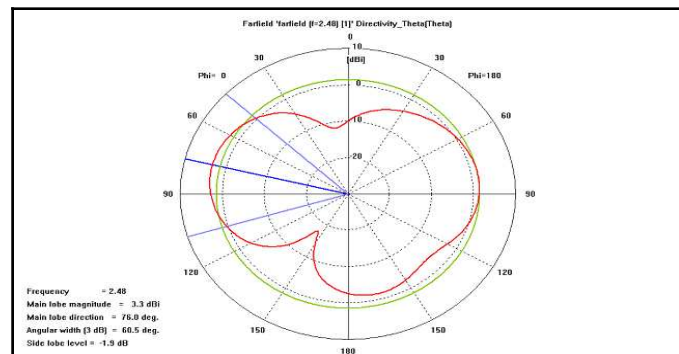


Figure 11: The radiation pattern of the vertical plane ($\Phi = 0^\circ$).

the x-axis, 18 mm on the z-axis, and 36 mm on the y-axis. The antenna length is 32 mm with 1 mm diameter. The CST Microwave Studio system calculates the expected radiation pattern for the model in three dimensions. Figure 8 shows the three-dimensional graph of the pattern for the mote in free space.

This specific output graph shows the directivity of the radiation pattern. If the gain is calculated for the window toward the x-axis, it will be 3.332 dBi as shown in the graph. For a better viewing of the results, the system created multiple cuts of the pattern at different angles.

Vertical and horizontal cuts were created and are shown in Figures 9 to 11. Figure 9 depicts the graph of the radiation pattern for horizontal cut plane calculations of the model. The graph is similar to the graph in Figure 4, which was created from real measurements in the Anechoic Chamber. The differences between the measurements (Figures 4 to 7) and simulations are due in part to inaccuracies in the experimental setup in the Anechoic Chamber. The simulation is evaluated over free space, where as the measurement is taken above a ground plane. Also, the MICAz model is assumed to be a perfect electric conductor in the CST.

Figure 10 depicts the graph of the radiation pattern for vertical cut plane calculations of the mote

model. The graph is similar to the graph in Figure 5, which was measured in the Anechoic Chamber. Again, minor differences in the null depths occur due to the experimental setup explained above. Also, the orientation of the graph has a 90° offset because of the different coordinate system reference between the experiment and simulator.

Figure 11 depicts the calculated graph of the radiation pattern for vertical cut of the mote model. The graph is different from the graphs in Figures 6 and 7, which were created from real measurements in the Anechoic Chamber. Figures 6 and 7 resulted from the two rotated positions according to Figures 3.c, and 3.d. If rotated appropriately, they should agree with the result in Figure 11. However, the nulls are deeper in the simulated pattern because of the free space environment and perfectly conducting material.

Comparing the results of experiment and simulation shows the asymmetry of the radiation pattern in the free space model. The fact that there are no external factors in the free space model implies that those irregularities are characteristics of the mote antenna itself. The asymmetrical pattern is a well-known phenomenon that occurs when electrically small antennas are mounted on small objects. The end user should plan the deployment with respect to the irregularity issue.

5 Conclusion

The objective of our work is to provide an in-depth analysis of the radio pattern of the MICAz mote. Results indicate that random deployment can have motes that are tilted in different orientations. Each orientation will give a different radio pattern which is not circular but instead having side lobes and nulls. Researchers should incorporate the non-ideal radio pattern of sensor nodes when designing new networking protocols and coverage algorithms. Otherwise, a portion of the network may become disjointed.

Acknowledgements: The authors would like to thank Professor David Jenn and Mr. Bob Broadston at Naval Postgraduate School for their help.

References:

- [1] G. Zhou, T. He, S. Krishnamurthy, and J. A. Stankovic, "Impact of Radio Irregularity on Wireless Sensor Networks," *MobiSYS 2004*, Boston, Massachusetts, June 2004.
- [2] D. Kotz, C. Newport, and C. Elliott, "The mistaken axioms of wireless-network research," *Dartmouth College Computer Science Technical Report TR2003-467*, July 18, 2003.
- [3] Z. Zhong, S. Das, and H. Gupta, "Variable Radii connected sensor cover in sensor networks," *IEEE SECON 2004*, pp. 387 - 396, Santa Clara, California, 2004.
- [4] P. Gupta and P. R. Kumar, "Critical power for asymptotic connectivity in wireless networks," *Stochastic Analysis, Control, Optimization and Applications: A Volume in Honor of W. H. Fleming, W. M. McEneaney, G. Yin, and Q. Zhang*, pp. 547-566, Eds. Boston, Massachusetts: Birkhauser, 1998.
- [5] M. Sanchez, P. Manzoni, and Z. J. Haas, "Determination of critical transmission range in ad hoc networks," *Multiaccess, Mobility and Teletraffic for Wireless Communications Workshop*, Venice, Italy, October 1999.
- [6] E. H. Callaway Jr., "Wireless Sensor Networks, Architecture and Protocols," Auerba Publications, CRC Press, Boca Raton, Florida, 2003.
- [7] T. S. Rappaport, "Wireless Communications Principles and Practice," pp. 105-253, Prentice Hall, Upper Saddle River, New Jersey, Second Edition.